

Electronic excitation spectra of furan and pyrrole: Revisited by the symmetry adapted cluster–configuration interaction method

Jian Wan, Jaroslaw Meller, Masahiko Hada, Masahiro Ehara, and Hiroshi Nakatsuji^{a)}

Department of Synthetic Chemistry and Biological Chemistry, Graduate School of Engineering, Kyoto University, Sakyo-ku, Kyoto 606-8501, Japan

(Received 20 June 2000; accepted 17 August 2000)

Electronic excitation spectra of furan and pyrrole are reinvestigated by the symmetry-adapted cluster configuration-interaction method. The 47 and 46 lowest singlet and triplet electronic states are computed for furan and pyrrole, respectively. Two series ($1a_2$ and $2b_1$) of low-lying Rydberg states and the valence π – π^* excited states strongly influence each other in both furan and pyrrole. The present calculations give detailed and satisfactory theoretical assignments of the vacuum ultraviolet spectra and the electron energy-loss spectra of the two molecules. The similarities and differences in the electronic excitations between furan and pyrrole are discussed in detail. The accuracy and assignments of recent theoretical studies, i.e., complete active space second-order perturbation, multireference Møller–Plesset perturbation, second-order algebraic-diagrammatic construction, multireference double configuration interaction, and CC3, are compared. © 2000 American Institute of Physics. [S0021-9606(00)30842-X]

I. INTRODUCTION

Furan and pyrrole are so-called five-membered six π -electron aromatic ring molecules in which the heteroatoms oxygen and nitrogen donate two π electrons and each of the four carbon atoms supplies one π electron. The electronic spectra of furan and pyrrole have been the subjects of many experimental and theoretical studies.^{1–29} The interest in these molecules is not surprising, considering the importance of these molecules as fundamental units in many important biological molecules. Further, recently, the calculations of their electronic excitation spectra have been considered as benchmarks for theoretical studies of excited states. The representative theoretical studies have been carried out so far by Nakatsuji *et al.*²¹ in 1985, Serrano-Andres *et al.*²² in 1993, Palmer and co-workers^{23,24} in 1995 and 1998, Trofimov and Schirmer^{26,27} in 1997, and Christiansen and co-workers^{28,29} in 1998 and 1999.

On the experimental side,^{1–15,23,24} three types of electronic excitation spectra were measured for furan and pyrrole: the vacuum ultraviolet (VUV) spectrum, electron energy-loss (EEL) spectrum, and ultraviolet photoelectron spectrum. These spectra provide information regarding singlet valence- and Rydberg-excited states, optically forbidden transitions such as triplet excitations, and ionization potentials, respectively.

On the other hand, the previous *ab initio* quantum theoretical investigations^{16–29} have demonstrated the underlying difficulties in calculating vertical excited states of furan and pyrrole. One is strong valence–Rydberg mixing. Calculations based only on the valence basis are obviously inadequate and this is a main reason for the failure of early semiempirical studies and early *ab initio* studies. Second, the roles of electron correlations are crucial. Accurate and reliable results are

obtained only by sophisticated electron-correlation methods for ground and excited states. Third, dynamic polarization of the σ electrons occurs strongly for some electronic excitations. Fourth, all of the previous three factors interact rather strongly in furan and pyrrole.

As observed from the experimental excitation spectra of furan and pyrrole (Figs. 3 and 4), the peaks are broad and complicated for the existence of many valence- and Rydberg-excited states and their vibrational structures. Generally band maxima and vertical excitation energies differ substantially: even for Rydberg states the deviation exceeds 0.2 eV in some cases.²⁷ This point should be kept in mind when trying to do an assignment and judge the accuracy of calculations.

Among the previous *ab initio* theoretical studies on furan and pyrrole, the symmetry adapted cluster (SAC) and SAC–configuration interaction (SAC–CI) study²¹ was a pioneering work, but due to the computational resources available at that time, the rather limited basis sets and relatively small active space impaired the quality of the results. In the later complete active space second-order perturbation (CASPT2),²² multireference Møller–Plesset (MRMP)²⁵ perturbation, second-order algebraic-diagrammatic construction ADC(2),^{26,27} and a hierarchy of coupled cluster model (coupled-cluster single double, CC3)^{28,29} studies, fairly large basis sets were used: the atomic natural orbital basis set contracted to $[4s3p1d/2s1p]$ and augmented by ring-centered diffuse s , p , and d functions in CASPT2, Dunning's cc-pVTZ basis set augmented by charge-centered $3s$, $3p$, and $3d$ Rydberg functions in MRMP, cc-pVDZ augmented by atom-centered diffuse functions and molecule-centered diffuse functions in ADC(2), and cc-pVTZ augmented by atom-centered diffuse functions and molecule-centered diffuse functions in CC3.

However, there are still many inconsistencies among the results of these recent high-level theoretical studies with

^{a)} Author to whom correspondence should be addressed; electronic mail: hiroshi@sbchem.kyoto-u.ac.jp

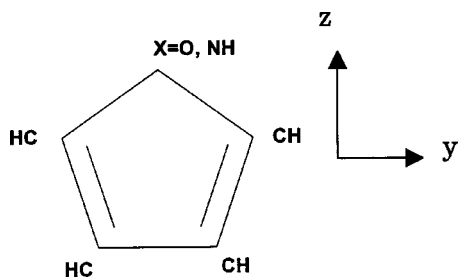


FIG. 1. Furan and pyrrole (C_4H_4X , $X=O, NH$).

large basis sets. For example, the CASPT2 and MRMP methods, which use a complete active space self-consistent field reference function, gave very similar computational results for furan and proposed a relatively reasonable interpretation of the singlet valence excitations lying lower than 7.8 eV, whereas, for pyrrole, they gave quite different results (0.51 eV difference) for the lowest valence excitation of 1B_2 symmetry, which was assigned to the first band of the VUV spectrum. For the same band, the ADC(2) studies made a conclusion that there was no valence excitation of 1B_2 symmetry in this region, which was explained solely by the Rydberg transitions. Recently, the fourth $\pi-\pi^*$ valence transition, $V'({}^1B_2)$, was identified by Palmer *et al.*²³ as an absorption peak at 8.7 eV in the VUV spectrum of furan with the aid of multireference multiroot CI multireference double configuration interaction (MRDCI) calculations. CASPT2 calculated this state at 8.38 eV with an intensity of 0.27, and MRMP did not visit this region. The CC3 estimated the corresponding state at an energy region higher than 9 eV.

On the other hand, since pyrrole differs from furan only by the substitution of an O atom by a N–H group, we would expect the electronic structures and excitation spectra of the two molecules to be similar. For example, the general profiles of VUV spectra of the two molecules^{23,24} are very similar in that they have two main intense and broad bands; the first is located at around 5.5–7 eV, and the second is more intense and located between 7.0 and 8.8 eV. However, an obvious difference exists in the spectra of pyrrole and furan, i.e., there is a weaker central band near 7 eV in the spectrum of pyrrole. The similarities and differences in the electronic excitation spectra of furan and pyrrole, and the uncertainties in the assignments of the valence and Rydberg excitations in the spectra of furan and pyrrole have motivated us to reinvestigate them using the SAC/SAC–CI method. In Sec. II we outline the computational details. Calculated results and discussion are presented in Sec. III. A summary is given in Sec. IV.

II. COMPUTATIONAL DETAILS

The experimentally determined ground-state equilibrium geometries³⁰ for furan and pyrrole with C_{2v} symmetry illustrated in Fig. 1 were commonly used for both ground and excited states, so that the calculated excitation energies are vertical in nature.

In the present calculations, we have used Dunning's augmented correlation consistent basis set AUG-cc-pVDZ³¹ for O, N and C atoms, and cc-pVDZ³² for H atoms. For the

molecule-centered Rydberg functions, we have used a set of diffuse functions ($3s3p3d$) selected from the studies of Kaufmann *et al.*,³³ and placed them on the molecular center of gravity. These are the same as those used by Trofimov and Schirmer.^{26,27} The total number of basis functions is 175 in furan and 180 in pyrrole. This type of augmented basis is believed to be adequate for describing widely different electronic structures of molecules in the ground state, singlet and triplet valence and Rydberg excited states, describing diffuse character and differential correlation effects. The number of Hartree–Fock canonical orbitals, calculated by the GAUSSIN98 package,³⁴ is 175, consisting of 18 occupied and 157 virtual orbitals in furan, and 180, consisting of 18 occupied and 162 virtual orbitals in pyrrole. The self-consistent field (SCF) occupied valence orbitals and some important virtual orbitals of furan and pyrrole are shown in Table I, respectively, together with their orbital energies, symmetries, and characters.

The details of the SAC/SAC–CI theory have been presented elsewhere.^{35–41} The SAC/SAC–CI calculations were done using the local version of the SAC–CI module.⁴¹ In all of the present SAC/SAC–CI calculations, the active space consists of 13 occupied orbitals and 157 and 162 virtual orbitals in furan and pyrrole, respectively: Only the $1s$ core molecular orbitals are frozen. The details of the SAC/SAC–CI calculations are exactly the same as those recently reported for cyclopentadiene.⁴²

Table II shows the previous²¹ and present SAC/SAC–CI computational details on furan and pyrrole. Note that, 15 years ago, SAC/SAC–CI was the only sophisticated theory for calculating the molecular excited states. The computational resources were quite different from those available now: The available main memory, disk space, and computational time were very limited, although the previous calculations were certainly “big” by the standard of that time. But now, we can use a much better basis set and a much larger active space than those in the previous SAC/SAC–CI studies. This greatly improves the calculated results, even though the basic method used is the same, i.e., the SAC/SAC–CI method. Improvements in the SAC/SAC–CI program, algorithm, etc., are also important, but when we do the comparisons shown in Table II, we are strongly convinced that advances in computer technology over the past 15 years play the greatest role in the present improvement.

III. RESULTS AND DISCUSSION

In the four π -orbital approximation, the two occupied orbitals $2b_1(\pi_2)$ and $1a_2(\pi_3)$, and the two virtual orbitals $3b_1(\pi_4^*)$ and $2a_2(\pi_5^*)$ illustrated in Fig. 2 give rise to four singlet $\pi-\pi^*$ transitions: $\pi_3\rightarrow\pi^*(V)$ and $\pi_2\rightarrow\pi^*(V')$. These four transitions $V({}^1B_2)$, $V'({}^1A_1)$, $V({}^1A_1)$, and $V'({}^1B_2)$ are expected to lie below the first ionization potential (IP₁) 8.883 eV in furan and 8.21 eV in pyrrole, and would give absorption bands in the range of 5.5–8.8 eV.

In order to distinguish valence and Rydberg-type transitions, we use some properties discussed in our recent paper.⁴² First, we take advantage of the fact that the A_2 and B_1 Rydberg states are not perturbed by the valence $\pi-\pi^*$

TABLE I. Hartree–Fock occupied molecular orbitals (MOs) and some important unoccupied MOs of furan and pyrrole. σ and π stand for valence character and Ryd stands for Rydberg character.

MOs	Symmetry		Orbital energy (eV)		Nature	
	Furan	Pyrrole	Furan	Pyrrole	Furan	Pyrrole
Occupied						
Cores						
6	$4a_1$	$4a_1$	-39.820	-35.263	$\sigma(1s)$	$\sigma(1s)$
7	$5a_1$	$5a_1$	-29.602	-28.470	$\sigma(2s)$	$\sigma(2s)$
8	$3b_2$	$3b_2$	-27.409	-26.621	$\sigma(2s)$	$\sigma(2s)$
9	$4b_2$	$6a_1$	-22.032	-21.711	$\sigma(2s)$	$\sigma(2s)$
10	$6a_1$	$4b_2$	-21.314	-20.913	$\sigma(2s)$	$\sigma(2s)$
11	$7a_1$	$7a_1$	-20.170	-20.074	$\sigma(2p)$	$\sigma(2p)$
12	$1b_1$	$8a_1$	-17.230	-16.181	π_1	$\sigma(2p)$
13	$5b_2$	$5b_2$	-16.621	-15.888	$\sigma(2p)$	$\sigma(2p)$
14	$6b_2$	$1b_1$	-15.694	-15.430	$\sigma(2p)$	π_1
15	$8a_1$	$6b_2$	-15.451	-14.861	$\sigma(2p)$	$\sigma(2p)$
16	$9a_1$	$9a_1$	-14.732	-14.411	$\sigma(2p)$	$\sigma(2p)$
17 (next highest occupied molecular orbital)	$2b_1$	$2b_1$	-10.835	-9.454	π_2	π_2
18 (highest occupied molecular orbital)	$1a_2$	$1a_2$	-8.702	-8.054	π_3	π_3
Unoccupied						
19 (lowest unoccupied molecular orbital)	a_1	a_1	0.047	0.041	<i>s</i> -Ryd	<i>s</i> -Ryd
20	b_2	a_1	0.162	0.146	<i>p_y</i> -Ryd	<i>s/p_z</i> -Ryd
21	a_1	b_2	0.166	0.164	<i>s/p_z</i> -Ryd	<i>p_y</i> -Ryd
23	a_1	a_1	0.201	0.207	<i>s/d</i> -Ryd	<i>s/d</i> -Ryd
26	a_2	b_1	0.355	0.359	<i>d_{xy}</i> -Ryd	<i>d_{xz}</i> -Ryd
27	a_1	a_2	0.360	0.360	<i>s/d</i> -Ryd	<i>d_{xy}</i> -Ryd
29	a_1	a_1	0.484	0.447	<i>s/d</i> -Ryd	<i>s/d_{yz}</i> -Ryd
30	b_2	b_2	0.544	0.553	<i>p_y</i> -Ryd	<i>p_y</i> -Ryd
32	b_1	b_1	0.589	0.596	<i>p_x</i> -Ryd	<i>p_x</i> -Ryd
33	b_2	a_1	0.951	0.945	<i>d_{yz}</i> -Ryd	<i>s/d</i> -Ryd
35	a_1	a_1	0.990	0.970	<i>s/d</i> -Ryd	<i>s/d</i> -Ryd
36	a_2	b_1	1.002	1.012	<i>d_{xy}</i> -Ryd	<i>d_{xz}/p_x</i> -Ryd
38	b_1	a_2	1.011	1.017	<i>d_{xz}/p_x</i> -Ryd	<i>d_{xy}</i> -Ryd
39	b_2	a_1	1.396	1.376	<i>p_y</i> -Ryd	<i>s/p_z</i> -Ryd
40	a_1	b_2	1.432	1.423	<i>s/p_z</i> -Ryd	<i>p_y</i> -Ryd
41	b_1	b_1	1.499	1.519	<i>p_x</i> -Ryd	<i>p_x</i> -Ryd
42	a_1	a_1	1.874	1.876	<i>s/d</i> -Ryd	<i>s/d</i> -Ryd
46	b_1	b_1	2.286	2.304	<i>d_{xz}/p_x</i> -Ryd	<i>d_{xz}/p_x</i> -Ryd
48	b_1	a_1	3.439	3.436	π^*	σ_s/d -Ryd
50	b_2	b_2	3.587	3.666	<i>p_y</i> -Ryd	<i>p_y</i> -Ryd
52	b_2	b_1	3.627	3.787	σ_{py}	π^*
53	a_2	a_2	4.043	4.145	π^*	π^*
57	b_1	a_1	4.837	4.920	π^*	σ_s/d -Ryd
59	a_1	b_1	4.909	5.149	σ_s/d -Ryd	π^*
61	b_1	a_2	6.298	6.054	π^*	π^*
62	a_1	b_1	6.888	6.465	σ_s	π^*
64	a_2	b_1	6.988	6.852	π^*	π^*
66	b_1	a_2	8.258	7.254	π^*	π^*

transitions due to the symmetry constraint. We then use the expectation values of the second moments of the charge distribution $\langle r^2 \rangle$, and its components $\langle x^2 \rangle$, $\langle y^2 \rangle$, and $\langle z^2 \rangle$. In addition, the oscillator strength has also been used by several authors as an indicator to compare valence and Rydberg characters.^{23,24,26,27} We will use all of them to analyze our SAC–CI results.

A. Furan

The calculated SCF energy of furan is $-228.654\,184$ hartrees. The SAC ground-state energy is $-229.070\,173$ hartrees, and the correlation energy is $-0.415\,988$ hartrees. The

corresponding previous values were $-228.557\,15$, $-228.810\,55$, and $-0.253\,40$ hartrees, respectively.

The singlet vertical excitation energies calculated by the SAC–CI method are given in Table III, which also shows the oscillator strength $[f(r)]$ and the second moment of each excited state. In Table IV, the present SAC–CI singlet and triplet excitation energies are compared with the experimental values, and with the results obtained by CASPT2, MRDCI, ADC(2), and CC3. Since for furan the MRMP results are quite similar to those for CASPT2, they are not given in Table IV. Figure 3 shows a comparison of the experimental VUV spectrum²³ and the theoretical SAC–CI spectrum of furan.

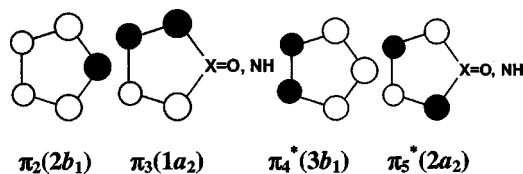
TABLE II. Comparison of the previous and present SAC/SAC-CI computational conditions for furan and pyrrole.

	Previous (Ref. 6)		Present		
Basis sets	DZ+Rydberg O, N and C: [4s2p] H: [2s] Rydberg (2s2p1d) on the molecular center of gravity		AUG-cc-pVDZ+Rydberg O, N and C: AUG-cc-pVDZ H: cc-pVDZ Rydberg (3s3p3d) on the molecular center of gravity		
Active space					
Furan	67 ^a [5 ^b ,51 ^c]		175 ^a [5 ^b ,170 ^c]		
Pyrrole	69 ^a [5 ^b ,53 ^c]		180 ^a [5 ^b ,175 ^c]		
Energy threshold for perturbation selection (PS)	$\lambda_g = 4.0 \times 10^{-5}$, $\lambda_e = 5.0 \times 10^{-5}$		$\lambda_g = 1.0 \times 10^{-5}$, $\lambda_e = 1.0 \times 10^{-6}$		
Dimension of linked operators after PS					
		Singlet	Triplet	Singlet	Triplet
	$A_1(G)^d$	2456		17 010	
	A_1	1896	2496	61 287	65 942
Furan	A_2	2260	2425	58 006	69 327
	B_1	2352	2017	106 049	49 416
	B_2	1805	2379	60 292	59 803
	$A_1(G)^d$	2457		16 437	
Pyrrole	A_1	1841	2515	67 165	71 068
	A_2	1883	2199	72 433	88 101
	B_1	1913	2487	89 004	88 690
	B_2	1758	2701	66 404	65 683

^aThe total number of MOs.^bThe number of frozen orbitals. 5 means "1s core".^cThe size of the active space, (occupied MO plus unoccupied MO).^dSAC ground state.

1. Singlet valence excited states

The first band system occurs in the region of 5.5–7.0 eV of the VUV spectrum. The maximum of this band lies at 6.04 eV (peak I in Fig. 3), which was assigned to the valence $\pi-\pi^*$ transition $V(^1B_2)$ by Palmer *et al.*²³ In addition, Flicker *et al.*⁸ observed the intensity maximum of a broad transition at 6.06 eV using electron impact spectroscopy and assigned it to $\tilde{X}^1A_1 \rightarrow ^1B_2$. In our present SAC-CI calculations, the excitation energy of the 1^1B_2 state is computed at 6.40 eV with an oscillator strength of 0.1852: it clearly represents the most intense feature of peak I. The second moment $\langle r^2 \rangle$ is 92.5358 a.u.², which defines it as a valence excited state, even if it is somewhat more diffuse than the ground state ($\langle r^2 \rangle = 64.6624$ a.u.²) due to valence-Rydberg mixing. The nature of the 1^1B_2 state is mainly the $\pi_3-\pi^*$ (18→48) excitations mixed with the Rydberg transitions (18→41), (18→32), and (18→46), etc. We would like to assign the first peak at 6.06 eV to the 1^1B_2 state. The exci-

FIG. 2. Two highest occupied π orbitals and two lowest unoccupied π^* orbitals of furan and pyrrole.

tation energies of the 1^1B_2 state were calculated to be 6.04, 6.76, 5.95, 6.37, and 6.35 eV by CASPT2, MRDCI, MRMP, ADC(2), and CC3, respectively. The corresponding oscillator strengths are 0.1543, 0.183, 0.158, 0.148, and 0.144, respectively. When we estimate the accuracy of these theoretical results, we should take into account the difference between the vertical excitation energy and the peak maximum. For example, it has been reported²⁸ that the difference between the vertical and the maximum peak excitation energies is at least 0.11 eV for the $^1B_{2u}$ valence excited state of benzene.

The region of greatest intensity in the VUV spectrum occurs from approximately 7.2 to 8.4 eV, with an intensity maximum at 7.8 eV (peak II in Fig. 3), to which the valence transition $V(^1A_1)$ has been assigned by most experimental and theoretical studies. Our present results calculated the 6^1A_1 state to lie at 8.34 eV above the ground state with an intensity of 0.4826. It is clearly related to the most intense feature of peak II. Its second moment $\langle r^2 \rangle$ is 97.5047 a.u.², which shows that it is a valence excited state, although it is somewhat more diffuse than the ground state due to slight valence-Rydberg mixing. The nature of the 6^1A_1 state is a mixing of $\pi_3-\pi^*$ (18→53) and $\pi_2-\pi^*$ (17→48) excitations and the Rydberg transitions (17→46) and (17→38), etc. Based on these results, we assign the 6^1A_1 state as the main component of the $V(^1A_1)$ transition. Note that the nature of the 6^1A_1 state is mixing of $\pi_3-\pi^*$ and $\pi_2-\pi^*$

TABLE III. Calculated excitation energies (in eV), second moments, and main configurations by the SAC/SAC-CI method for furan.

State	Nature ^a	ΔE^b	Pol ^c	$f(r)$	Second moment			
					$\langle x^2 \rangle$	$\langle y^2 \rangle$	$\langle z^2 \rangle$	$\langle r^2 \rangle$
1 ¹ A ₁	Ground	0.0		0	24.6628	18.4772	21.5224	64.6624
1 ¹ A ₂	3s-R	5.99		Forbid	42.5477	34.8039	38.6635	116.0150
1 ¹ B ₂	V-mix	6.40	y	0.1852	42.7817	23.8893	25.8647	92.5358
1 ¹ B ₁	3p _y -R	6.45	x	0.0313	37.0420	65.4676	34.1141	136.6238
2 ¹ A ₂	3p _z -R	6.66		Forbid	40.3748	33.2618	75.0431	148.6797
2 ¹ A ₁	V	6.79	z	0.0000	25.9881	20.0661	22.9068	68.9609
2 ¹ B ₂	3p _x -R	6.82	y	0.0158	65.3598	26.3912	37.7410	129.4920
3 ¹ A ₂	3d-R	7.04		Forbid	41.6107	68.7722	33.1252	143.5080
2 ¹ B ₁	3d _{yz} -R	7.14	x	0.0005	37.0320	60.9984	64.9757	163.0060
4 ¹ A ₂	3d-R	7.27		Forbid	52.6200	30.0711	89.0683	171.7594
3 ¹ A ₁	3d _{xy} -R	7.36	z	0.0001	91.1382	80.6382	40.2160	211.9923
3 ¹ B ₁	3s'-R	7.45	x	0.0292	45.5458	47.8471	45.2990	138.6919
5 ¹ A ₂	4s-R	7.50		Forbid	153.8467	90.5160	99.9118	344.2746
3 ¹ B ₂	3d _{xz} -R	7.51	y	0.0194	108.2377	40.0669	97.4018	245.7064
4 ¹ B ₁	4p _y -R	7.67	x	0.0008	94.2931	226.6794	90.7120	411.6845
4 ¹ B ₂	4p _x -R	7.71	y	0.0010	246.8240	86.1320	96.7509	429.7070
6 ¹ A ₂	4p _z -R	7.72		Forbid	104.4467	91.4211	255.1376	451.0054
7 ¹ A ₂	4d-R	7.85		Forbid	113.9521	256.0963	75.7213	445.7697
5 ¹ B ₁	4d _{yz} -R	7.89	x	0.0000	79.7302	185.1881	190.2943	455.2126
8 ¹ A ₂	4d-R	7.93		Forbid	121.5102	76.7263	269.3098	467.5463
4 ¹ A ₁	4d _{xy} -R	7.99	z	0.0002	211.5385	200.0038	80.1687	491.7110
9 ¹ A ₂	5s-R	8.04		Forbid	366.5189	246.8423	260.1989	873.5601
5 ¹ B ₂	4d _{xz} -R	8.07	y	0.0069	225.2252	78.9295	209.5113	513.6660
6 ¹ B ₁	3p _z '-R	8.07	x	0.0006	44.3096	48.8139	78.7930	171.9166
5 ¹ A ₁	3p _x '-R	8.14	z	0.0205	83.4876	39.7525	37.0449	160.2850
7 ¹ B ₁	5p _y -R	8.18	x	0.0023	145.3949	381.7329	142.6457	669.7735
6 ¹ B ₂	5p _x -R	8.19	y	0.0016	389.8390	133.7052	144.3590	667.9031
10 ¹ A ₂	5p _z -R	8.21		Forbid	147.3133	136.8059	392.3236	676.4428
6 ¹ A ₁	V-mix	8.34	z	0.4826	38.4469	26.9042	32.1536	97.5047
8 ¹ B ₁	5d _{yz} -R	8.47	x	0.0017	54.9059	120.4527	100.1038	275.4624
9 ¹ B ₁	3d'-R	8.54	x	0.0095	62.5576	135.8883	117.9192	316.3651
10 ¹ B ₁	3d'-R	8.67	x	0.0292	57.9288	47.8102	74.4203	180.1593
7 ¹ A ₁	5d _{xy} -R	8.69	z	0.0035	184.2435	173.1875	71.3490	428.7800
7 ¹ B ₂	5d _{xz} -R	8.75	y	0.0222	168.8308	63.9795	157.0494	389.8597
8 ¹ B ₂	3d' _{xy} -R	8.79	y	0.0243	88.9270	68.6441	50.3966	207.9677
11 ¹ B ₁	3d'-R	8.87	x	0.0048	38.4421	52.1882	72.9737	163.6040
8 ¹ A ₁	4s'-R	8.95	x	0.0036	135.2292	98.2036	116.8031	350.2359
12 ¹ B ₁	3d' _{xz} -R	8.95	z	0.0703	104.0758	41.4103	97.6589	243.1450
9 ¹ B ₂	V-mix	9.08	y	0.1662	56.3822	41.8921	32.1471	130.4213
13 ¹ B ₁	4'p _z -R	9.15	x	0.0003	111.3931	93.3319	239.8221	444.5471
1 ³ B ₂	V	4.39		...	25.0331	18.3365	22.6064	65.9760
1 ³ A ₁	V	5.63		...	25.2181	19.2344	22.5002	66.9527
1 ³ A ₂	3s-R	5.98		...	43.0576	34.1056	37.2876	114.4508
1 ³ B ₁	3p _y -R	6.52		...	37.8233	67.2748	34.9733	140.0714
2 ³ B ₂	3p _x -R	6.66		...	73.5041	29.5236	34.6416	137.6693
2 ³ A ₂	3p _z /s-R	6.68		...	39.7699	33.0344	74.0609	146.8652
2 ³ A ₁	V	7.10		...	29.0880	22.2528	23.5868	74.9276
2 ³ B ₁	3d _{yz} -R	7.21		...	38.2497	64.9995	68.9878	172.2370

^aV and R denote, respectively, valence and Rydberg excited state. For details see the text.^bTransition energy.^cPolarization direction of the transition moment.

transitions, and the notation $V(^1A_1)$, based the simple four π -orbital model, is inadequate because “V” denotes only $\pi_3-\pi^*$ type transitions.

CASPT2 computed the 4^1A_1 state at 7.74 eV with an intensity of 0.4159, and it was reported²¹ that the appearance of intruder states in CASPT2 wave function renders an uncertainty of about 0.2 eV to this state. MRDCI computed this state at 8.324 eV with an intensity of 0.476. MRMP com-

puted the 4^1A_1 state at 7.69 eV with an oscillator strength of 0.494, ADC(2) at 8.16 eV with an oscillator strength of 0.308, CC3 at 8.35 eV with an oscillator strength of 0.350.

Recently, Palmer *et al.*²³ assigned an absorption peak at 8.7 eV in their VUV spectrum (peak III in Fig. 3) to the valence excitation $V'(^1B_2)$ with the aid of MRDCI calculated results: 9.422 eV with an intensity of 0.197. In their studies, the relative intensities were important for relating

TABLE IV. SAC–CI results compared with the experimental excitation energies and other theoretical results for furan.

State	Nature ^a	SAC–CI		Expt. ^c	CASPT2 ^d		CC3(CCSD) ^e		MRDCI ^g		ADC(2) ⁱ	
		$f(r)$	ΔE^b		ΔE	State	ΔE^f	Nature	ΔE^h	Nature	ΔE	Nature
1 ¹ A ₂	3s–R	Forbid	5.99	5.91	5.92	1 ¹ A ₂	6.11	3s(¹ A ₂)	5.950	3s(¹ A ₂)	5.86	3s(¹ A ₂)
1 ¹ B ₂	V	0.1852	6.40	6.04	6.04	1 ¹ B ₂	6.35	V(¹ B ₂)	6.759	V(¹ B ₂)	6.37	V(¹ B ₂)
1 ¹ B ₁	3p _y –R	0.0313	6.45	6.47	6.46	1 ¹ B ₁	6.64	3p _y (¹ B ₁)	6.659	3p _x (¹ B ₂)	6.35	3p(¹ B ₁)
2 ¹ A ₂	3p _z –R	Forbid	6.66	6.61	6.59	2 ¹ A ₂	6.80	3p _z (¹ A ₂)			6.50	3p(¹ A ₂)
2 ¹ A ₁	V	0.0000	6.79		6.16	2 ¹ A ₁	6.61	V(¹ A ₁)	6.024	V(¹ A ₁)	6.70	V(¹ A ₁)
2 ¹ B ₂	3p _x –R	0.0158	6.82	6.75	6.48	2 ¹ B ₂	6.94	3p _x (¹ B ₂)	6.633	3p _y (¹ B ₁)	6.73	3p(¹ B ₂)
3 ¹ A ₂	3d–R	Forbid	7.04		7.00	3 ¹ A ₂	7.12	3d _z ² (¹ A ₂)				
2 ¹ B ₁	3d _{yz} –R	0.0005	7.14		7.15	2 ¹ B ₁					6.89	3d(¹ A ₂)
4 ¹ A ₂	3d–R	Forbid	7.27		7.22	4 ¹ A ₂					6.98	3d(¹ B ₁)
3 ¹ A ₁	3d _{xy} –R	0.0001	7.36	7.28	7.31	3 ¹ A ₁	7.32	3d _{yz} (¹ B ₁)	6.988	3d _{yz} (¹ B ₁)	7.22	3d(¹ A ₁)
3 ¹ B ₁	3s'–R	0.0292	7.45	7.38	7.21	3 ¹ B ₁	7.52	3s'(¹ B ₁)	7.143	3s'(¹ B ₁)	7.05	3s'(¹ B ₁)
5 ¹ A ₂	4s–R	Forbid	7.50								7.80	4s(¹ A ₂)
3 ¹ B ₂	3d _{xz} –R	0.0194	7.51	7.43	7.13	3 ¹ B ₂	7.58	3d _{xy} (¹ A ₁)	7.405	3d _z ² (¹ A ₂)	7.11	3d(¹ A ₂)
4 ¹ B ₁	4p _y –R	0.0008	7.67	7.52			7.70	4s(¹ A ₂)	7.594	4s(¹ A ₂)	7.30	4s(¹ A ₂)
4 ¹ B ₂	4p _x –R	0.0010	7.71	7.53			7.72	3d _{xz} (¹ B ₂)	7.750	3d _{xy} (¹ A ₁)	7.35	3d(¹ B ₂)
6 ¹ A ₂	4p _z –R	Forbid	7.72									
7 ¹ A ₂	4d–R	Forbid	7.85	7.70					7.824	4p _x (¹ B ₂)	7.48	4p(¹ B ₁)
5 ¹ B ₁	4d _{yz} –R	0.0000	7.89				7.90	4p _y (¹ B ₁)				
8 ¹ A ₂	4d–R	Forbid	7.93	7.79			7.94	4p _x (¹ B ₂)	7.652	4p _y (¹ B ₂)	7.53	4p(¹ B ₂)
4 ¹ A ₁	4d _{xy} –R	0.0002	7.99								7.51	4p(¹ A ₂)
9 ¹ A ₂	5s–R	Forbid	8.04								7.57	3P'(¹ A ₂)
											7.72	4d(¹ B ₁)
											7.87	4d(¹ B ₂)
5 ¹ B ₂	4d _{xz} –R	0.0069	8.07	8.01			8.26	4d _{xz} (¹ B ₂)			7.82	4d(¹ A ₁)
6 ¹ B ₁	3p _z '–R	0.0006	8.07	8.04			8.20	4d _{xy} (¹ A ₁)	7.563	4d _z ² (¹ A ₂)	7.66	4d(¹ A ₂)
									8.581	4d _{xy} (¹ A ₁)	7.72	4d(¹ A ₂)
									8.844	5s(¹ A ₂)	7.80	5s(¹ A ₂)
5 ¹ A ₁	3p _x '–R	0.0205	8.14	8.10			8.26	3p _x '(¹ A ₁)	8.148	3p _x '(¹ A ₁)	7.61	3p'(¹ B ₁)
7 ¹ B ₁	5p _y –R	0.0023	8.18	8.19			8.34	5p _y (¹ B ₁)	8.040	3p _z '(¹ B ₁)	7.96	5p(¹ B ₁)
6 ¹ B ₂	5p _x –R	0.0016	8.19	8.23			8.36	5p _x (¹ B ₂)			7.99	5p(¹ B ₂)
10 ¹ A ₂	5p _z –R	Forbid	8.21								7.71	3p'(¹ A ₁)
6 ¹ A ₁	V-mix	0.4826	8.34	7.8	7.74	4 ¹ A ₁	8.35	V(¹ A ₁)	8.324	V(¹ A ₁)	8.16	V(¹ A ₁)
8 ¹ B ₁	5d _{yz} –R	0.0017	8.47	8.32			8.52	5d _{xz} (¹ B ₂)				
9 ¹ B ₁	3d'–R	0.0095	8.54	8.34			8.50	5d _{xy} (¹ A ₁)			8.06	3d'(¹ B ₁)
10 ¹ B ₁	3d' _{yz} –R	0.0292	8.67	8.46					8.327	3d' _{yz} (¹ A ₁)	8.32	3d'(¹ B ₂)
7 ¹ A ₁	5d _{xy} –R	0.0035	8.69						8.359	3d' _{x-y} (¹ B ₁)	8.23	3d'(¹ B ₁)
7 ¹ B ₂	5d _{xz} –R	0.0222	8.75									
8 ¹ B ₂	3d' _{xy} –R	0.0243	8.79	8.77					8.936	3d' _{xy} (¹ B ₂)	8.51	3d'(¹ A ₁)
11 ¹ B ₁	3d'–R	0.0048	8.87						8.395	3d _z ² (¹ B ₁)		
8 ¹ A ₁	3d' _{xz} –R	0.0036	8.95									
12 ¹ B ₁	4s'–R	0.0703	8.95									
9 ¹ B ₂	V-mix	0.1662	9.08	8.7	8.38	V ¹ B ₂	>9	V(¹ B ₂)	9.422	V'(¹ B ₂)	8.64	V'(¹ B ₂)
13 ¹ B ₁	4'p _z –R	0.0003	9.15	8.96							8.41	4s'(¹ B ₁)
1 ³ B ₂	V	...	4.39	3.99	3.99				3.931		4.31	
1 ³ A ₁	V	...	5.63	5.15	5.15				5.282		5.50	
1 ³ A ₂	3s–R	...	5.98		5.86				6.682		5.81	
1 ³ B ₁	3p _y –R	...	6.52		6.42				9.077		6.31	
2 ³ B ₂	3p _x –R	...	6.66	~6.5					6.313			
2 ³ A ₂	3p _z /s–R	...	6.68						8.733			
2 ³ A ₁	V	...	7.10	~6.5					6.648			

^aV and R denote, respectively, valence and Rydberg excited state. For details see the text.^bTransition energy (in eV).^cExperimental data were taken from Refs. 21–25 and references therein.^dReference 21.^eReference 25.^fCC3 for valence and CCSD for Rydberg.^gReference 22.^hDifferent basis sets were used for valence and Rydberg.ⁱReference 24.

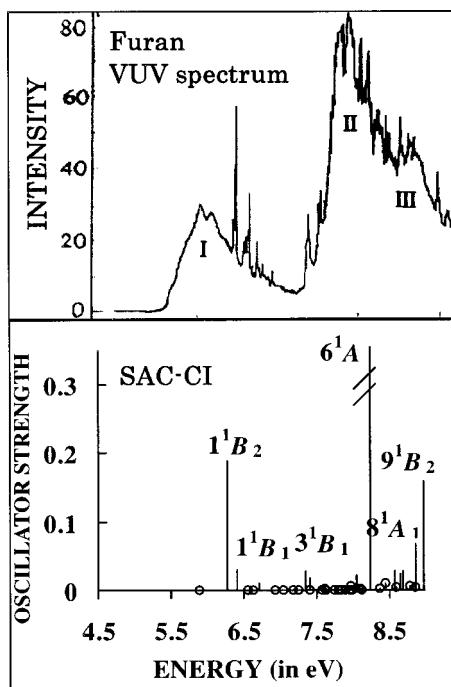


FIG. 3. VUV spectrum and SAC-CI theoretical spectrum of furan.

calculated results with experimental data when MRDCI results did not agree with the experimental data for the higher $\pi-\pi^*$ transitions. Our present results give the 9^1B_2 state at 9.08 eV with an intensity of 0.1662 in this region. The second moment $\langle r^2 \rangle$ of this state is 130.4213 a.u.², which clearly shows that this state has significant diffuse character. Its nature is mainly due to the $\pi_2-\pi^*$ (17→53) and (17→64) excitations $V'(^1B_2)$ mixed by the Rydberg transitions (17→26) and (17→36), etc. CASPT2 calculated this state at 8.38 eV with an intensity of 0.27. MRMP did not give this state. ADC(2) computed this state at 8.64 eV with an oscillator strength of 0.116. CC3 estimated this state to be above 9 eV and therefore outside of the energy range considered.

Finally, we discuss the valence excitation, $V'(^1A_1)$, which is expected to occur in the first band. However, contrary to the $V(^1B_2)$ valence excitation which has been relatively well established, the $V'(^1A_1)$ excitation is so complicated that it has not yet been reasonably assigned. There is a progression of weak peaks at 5.70, 5.80, 5.89, and 5.91 eV in the UV absorption spectrum. This was assigned to a Rydberg transition and its vibronic lines by Robin,¹⁵ and to the $V'(^1A_1)$ valence transition by Roebber *et al.*¹³ Palmer *et al.* stated that their recent work²³ supported the valence-type assignment because their MRDCI calculations gave the energy order $^1A_1 < ^1B_2$ for the two lowest valence transitions, although the numerical results for these two states changed greatly with different basis sets. The 1A_1 state was calculated at 6.024 eV with an intensity of 0.011, and the 1B_2 state was calculated at 6.759 eV with an intensity of 0.183 using the double zeta plus polarization (DZP) basis, and these two states were calculated at 6.63 and 6.88 eV, respectively, using the DZPR basis in a MRDCI study.²³ Note that the nature of the 2^1A_1 state in the MRDCI study is only $\pi_2 \rightarrow \pi^*$.

CASPT2 computed the 2^1A_1 state at 6.16 eV with an intensity of 0.0015, and its nature was reported to be a mixture of the configurations $2b_1 \rightarrow 3b_1$ and $1a_2 \rightarrow 2a_2$ and the double excitation of $[(1a_2)^2 \rightarrow (3b_1)^2]$. MRMP computed the 2^1A_1 state at 6.16 eV with an intensity of 0.0035, and its nature was almost the same as that by CASPT2, Rydberg mixing was also found. ADC(2) computed this state at 6.70 eV with an oscillator strength of 0.003. CC3 computed it to be 6.61 eV with an oscillator strength of 0.000. Our present calculations give the 2^1A_1 state at 6.79 eV with an oscillator strength of 0.0000. Its second moment $\langle r^2 \rangle$ is 68.9609 a.u.², which clearly defines it as a valence excited state, and its nature is a mixture of $\pi_2-\pi^*$ (17→48) and (17→61) and $\pi_3-\pi^*$ transitions (18→53) and (18→64). Double excitation makes a rather small contribution. Note that all of the above-mentioned theoretical methods, except MRDCI, gave an energy order of $^1B_2 < ^1A_1$. This implies that the first 1A_1 valence state should be located at a higher energy shoulder of the first band. Due to the very weak intensity of this valence transition, there is no obvious experimental evidence to confirm the theoretical results, and *vice versa*. However, in the case of thiophene, which will be discussed in a later paper,⁴³ the 2^1A_1 state has been well characterized with regard to both excitation energy and oscillator strength, in comparison with the experimental data of the VUV and magnetic circular dichroism spectra.

2. Singlet Rydberg states

The lowest singlet Rydberg transition has been assigned to the $1a_2 \rightarrow 3s$ Rydberg series. Robin¹⁵ first assigned the weak feature at 5.94 eV to the dipole-forbidden 1A_2 Rydberg state, and later Roebber *et al.*¹³ also assigned the weak peak at 5.91 eV to the $1a_2 \rightarrow 3s$ Rydberg state using multiphoton ionization spectroscopy (MPI). In the present calculations, the 1^1A_2 state is computed at 5.99 eV and its nature is a $3s$ -Rydberg transition. The CASPT2, MRDCI, MRMP, ADC(2), and CCSD methods computed this state at 5.92, 5.95, 5.84, 5.86, and 6.11 eV, respectively.

The group of transitions in the region 6.4–6.8 eV has usually been assigned to the $1a_2 \rightarrow 3p$ Rydberg series. Derrick and co-workers^{5,6} assigned the band with a 0–0 origin at 6.475 eV to the transition $1a_2 \rightarrow 3pb_2$. Cooper *et al.*¹² assigned 6.47 eV to the $3p$ Rydberg states in their MPI spectroscopy studies, which supported the results of Derrick and co-workers. Recently, the $3pb_2(^1B_1)$ assignment was questioned by Palmer *et al.*,²² who assigned 6.472 eV to the 1B_2 state on the basis of their MRDCI calculations. Our present calculations computed the 2^1B_2 state at 6.82 eV, well separated from the 1^1B_1 transition at 6.45 eV, which is consistent with the ADC(2) and CCSD results. Therefore, we assigned an observed transition at 6.47 eV to the $1a_2 \rightarrow 3p_y(^1B_1)$ Rydberg series.

The nature of the transition observed at 6.75 eV has been the subject of controversy.^{12,14,23} Cooper *et al.*¹² assigned it tentatively to the 1A_1 valence-type transition. This was criticized by Robin,¹⁵ and more recently, this peak at 6.75 eV was assigned to the $3p$ -Rydberg transition by Nyulaszi.¹⁴ Recently, Palmer *et al.*²³ convincingly proved the $3p$ -Rydberg origin of the 6.75 eV band, but assigned it to

$1a_2 \rightarrow 3p_y$ (1B_1) based on their MRDCI results. Taking into account the discussion on the 6.47 eV transition, we believe the 2^1B_2 state is a better candidate for the observed 6.75 eV transition, which is consistent with the ADC(2) and CCSD results. CASPT2 computed the 1^1B_1 and 2^1B_2 states at 6.46 and 6.48 eV, respectively, and assigned both of them to the 6.47 eV transition. MRMP computed the 1^1B_1 and 2^1B_2 state at 6.40 and 6.50 eV, respectively, and also assigned both of them to the 6.47 eV transition. Apparently, the observed 6.75 eV transition was overlooked by the CASPT2 and MRMP studies, which is rather misleading because no evidence for a second transition at 6.48 eV can be found in the experimental spectrum. In addition, we computed the dipole-forbidden 2^1A_2 state at 6.66 eV, which is a $1a_2 \rightarrow 3p_z$ Rydberg series.

Following the above-mentioned three $3p$ -Rydberg states, there is an experimentally identified Rydberg transition at 7.28 eV. This transition was interpreted as the $3d$ -Rydberg series,^{5,7,14} however, the spatial symmetry designation of this series is again not fully secure. Derrick and co-workers^{5,6} experimentally assigned the transition at 7.28 eV to the 3^1A_1 state. CASPT2 calculations gave the 2^1B_1 state at 7.15 eV and the 3^1A_1 state at 7.31 eV, and followed the assignment of Derrick and co-workers MRMP and ADC(2) also followed the choice of CASPT2: the 2^1B_1 and 3^1A_1 states were computed at 7.10 and 7.26 eV by MRMP, and at 6.98 and 7.22 eV by ADC(2), respectively. Recently, however, Palmer *et al.*²² assigned the observed 7.28 eV transition to the $3d$ (1B_1) state according to their MRDCI results: the 2^1B_1 state at 6.988 eV and the 3^1A_1 state at 7.75 eV. CCSD calculated the $3d_{yz}$ (1B_1) state at 7.32 eV and followed the assignment by Palmer *et al.* Our present results computed the 2^1B_1 ($3d_{yz}$) state at 7.14 eV, and the 3^1A_1 ($3d_{xy}$) state at 7.36 eV. The assignment to the $3d_{xy}$ (1A_1) state seems more natural, and therefore we assign the 7.28 eV transition to the 3^1A_1 ($3d_{xy}$) Rydberg series, as with CASPT2, MRMP, and ADC(2).

The next transition at 7.38 eV has usually been assigned to the $1b_1 \rightarrow 3s$ Rydberg series ($3s'$).^{5,12,23} Our present calculations gave the 3^1B_1 ($3s'$) state at 7.45 eV. CASPT2, MRDCI, MRMP, ADC(2), and CCSD calculations gave this state at 7.21, 7.143, 7.31, 7.05, and 7.52 eV, respectively.

Regarding the transitions at 7.43, 7.52, and 7.53 eV, MRDCI calculations assigned them to the dipole-forbidden transitions $1a_2 \rightarrow 3d$ (1A_2 , 7.405 eV), $1a_2 \rightarrow 4s$ (1A_2 , 7.594 eV) and the dipole-allowed transition $1a_2 \rightarrow 3d$ (1A_1 , 7.750 eV) states, respectively. ADC(2) studies assigned these three transitions to the $3d$ (1A_2 , 7.22 eV), $4s$ (1A_2 , 7.30 eV), and $3d$ (1B_2 , 7.35 eV) states, respectively. However, according to our present results, we prefer to tentatively assign them to 3^1B_2 ($3d_{xz}$, 7.51 eV), 4^1B_1 ($4p_y$, 7.67 eV), and 4^1B_2 ($4p_x$, 7.71 eV). Our present assignment of Rydberg transitions lower than 7.53 eV is consistent with the energy order and gap of the experimental data.

In the energy region higher than 7.53 eV, Rydberg transitions become increasingly dense, and the assignment of individual Rydberg transitions is more difficult. Therefore, the assignments of the experimental data higher than 7.53 eV given in Table IV are tentative.

3. Triplet excited states

The two lowest triplet transitions of furan have been well identified by electron energy-loss (EEL) spectroscopy^{8–10,23} at 3.99 and 5.2 eV, which are assigned to the 3B_2 and 3A_1 valence transitions, respectively. Our present calculations computed the 1^3B_2 state at 4.39 eV with a second moment of 65.9760 a.u.², and 1^3A_1 at 5.63 eV with a second moment of 66.9527 a.u.². The second moments of these two states clearly characterize them as valence excitations. The main configurations of 3B_2 are (18→48), (18→61), (18→57), etc., and those of 3A_1 are (17→48), (18→64), (18→53), (17→61), etc.

Recently, Palmer *et al.*²³ observed two higher triplet transitions at around 6.5 eV in their EEL spectrum study and assigned them to the 2^3A_1 and 2^3B_2 states. Our present calculations gave the $3p$ series of triplet Rydberg states in this energy region, 1^3B_1 ($3p_y$) at 6.52 eV, 2^3B_2 ($3p_x$) at 6.66 eV, and 2^3A_2 ($3p_z$) at 6.68 eV. The valence triplet excited state 2^3A_1 was given at 7.10 eV with the main configurations of (17→48), (18→53), (18→64), etc. These states are related to the two higher triplet transitions in the EEL spectrum.

B. Pyrrole

The SCF energy of pyrrole is -208.838 068 hartrees. The SAC ground-state energy is -209.218 937 hartrees, and the correlation energy is -0.380 869 hartrees. The corresponding previous values were -208.754 72, -208.993 36, and -0.238 64 hartrees, respectively.

The principal SAC-CI results for the singlet and triplet vertical excitation energies are shown in Table V, along with the oscillator strength [$f(r)$] and second moment of each excited state. In Table VI, the present SAC-CI singlet and triplet excitation energies are compared to the experimental values, and to the results obtained by CASPT2, MRMP, ADC(2), and CC3. Figure 4 shows a comparison of the experimental VUV spectrum²⁴ and the theoretical SAC-CI spectrum of pyrrole. Additionally, to interpret the similarities and differences between the VUV spectra of pyrrole and furan, the excitation energies, oscillator strengths, second moments, and main configurations of the valence excitations of the two molecules are compared in Table VII.

1. The first intense and broad band (5.2–6.6 eV) of the VUV spectrum

Our present calculations show that the first three 1B_2 states are computed at 5.88, 6.48, and 6.76 eV, respectively, with oscillator strengths of 0.0805, 0.0475 and 0.0789, respectively. The second moments of the three excited states are 132.1, 146.3, and 224.7 a.u.², respectively. It is difficult to distinguish these three states as valence excitation or Rydberg excitation by the second moments and oscillator strengths. However, we can use a simple hybrid model to give an interpretation. Since there are three configurations 1^1B_2 ($1a_2 \rightarrow 3p_x$), 2^1B_2 (valence $1a_2 \rightarrow \pi^*$), and 3^1B_2 ($1a_2 \rightarrow 3d_{xz}$) which are close in energy, we can assume that these three configurations ($1a_2 \rightarrow 3p_x$, π^* , and $3d_{xz}$) are strongly mixed with each other and then construct three new hybrid excited states 1^1B_2 ($1a_2$

TABLE V. Calculated excitation energies (in eV), oscillator strengths, and second moments of pyrrole.

State	Nature ^a	ΔE^b	Pol ^c	$f(r)$	Second moment			
					$\langle x^2 \rangle$	$\langle y^2 \rangle$	$\langle z^2 \rangle$	$\langle r^2 \rangle$
1 ¹ A ₁	Ground	0		0	26.3093	20.6830	18.3334	65.3256
1 ¹ A ₂	3s-R	5.11		Forbid	38.5385	31.6834	44.4993	114.7213
1 ¹ B ₁	3p _y -R	5.80	x	0.0211	40.1805	69.3496	35.1595	144.6895
2 ¹ A ₂	3p _z -R	5.81		Forbid	44.0000	38.9442	56.7104	139.6547
1 ¹ B ₂	3p _x -R	5.88	y	0.0805	70.6606	31.5707	29.9041	132.1354
2 ¹ B ₁	3s'-R	6.05	x	0.0005	39.1957	37.2409	43.7521	120.1888
3 ¹ A ₂	3d-R	6.38		Forbid	42.1899	78.4625	47.3118	167.9642
3 ¹ B ₁	3d _{yz} -R	6.39	x	0.0037	40.0846	64.5531	64.3982	169.0359
2 ¹ A ₁	V	6.41	z	0.0002	29.5900	24.3270	19.4281	73.3451
4 ¹ A ₂	3d-R	6.44		Forbid	70.1989	31.9981	57.5656	159.7626
2 ¹ B ₂	V-3d _{xz} -R	6.48	y	0.0475	68.3278	30.0456	47.9410	146.3143
3 ¹ A ₁	3d _{xy} -R	6.64	z	0.0000	95.7588	83.8498	37.4214	217.0300
4 ¹ B ₁	3p' _z -R	6.68	x	0.0266	44.3956	44.7269	61.0966	150.2190
5 ¹ A ₂	4s-R	6.71		Forbid	112.8202	79.8926	147.4559	340.1687
3 ¹ B ₂	3d _{xz} -R	6.76	y	0.0789	103.2229	41.5147	79.9981	224.7356
4 ¹ A ₁	3p' _x -R	6.86	z	0.0146	81.7840	39.3594	32.4668	153.6102
5 ¹ B ₁	4p _y -R	6.93	x	0.0029	103.5279	254.7510	99.6378	457.9166
6 ¹ A ₂	4p _z -R	6.95		Forbid	131.9602	107.6015	177.5677	417.1295
4 ¹ B ₂	4p _x -R	6.99	y	0.0020	244.7481	87.0448	89.8109	421.6038
7 ¹ A ₂	4d-R	7.11		Forbid	167.1016	189.0867	88.1108	444.2990
8 ¹ A ₂	4d-R	7.13		Forbid	105.1136	149.2357	231.5695	485.9187
6 ¹ B ₁	4d _{yz} -R	7.14	x	0.0001	86.5404	203.5861	194.1834	484.3100
5 ¹ A ₁	4d _{xy} -R	7.26	z	0.0041	216.4420	205.8745	77.9965	500.3131
7 ¹ B ₁	3d'-R	7.26	x	0.0018	49.2432	59.8176	59.5719	168.6327
5 ¹ B ₂	4d _{xz} -R	7.26	y	0.0119	209.6781	75.2864	199.8960	484.8605
9 ¹ A ₂	5s-R	7.27		Forbid	296.8269	230.0584	330.6280	857.5133
8 ¹ B ₁	3d'-R	7.34	x	0.0092	63.3648	73.0189	33.5406	169.9242
10 ¹ A ₂	5p _z -R	7.44		Forbid	195.3911	177.9971	371.4336	744.8217
9 ¹ B ₁	5p _y -R	7.44	x	0.0048	142.7447	373.8345	138.7340	655.3133
6 ¹ B ₂	5p _x -R	7.45	y	0.0020	390.0070	135.3600	136.3607	661.7277
6 ¹ A ₁	3d' _{xz} -R	7.49	z	0.0679	88.5856	41.1360	73.4847	203.2063
7 ¹ B ₂	3d' _{xy} -R	7.55	y	0.0052	100.2877	91.3482	37.2567	228.8926
10 ¹ B ₁	4s'-R	7.63	x	0.0000	115.5165	80.3642	149.7550	345.6358
11 ¹ B ₁	5d _{yz} -R	7.75	x	0.0002	83.3076	190.2939	187.5531	461.1546
7 ¹ A ₁	4'p _x -R	7.83	z	0.0020	243.7424	93.9043	89.3948	427.0415
8 ¹ A ₁	V-mix	7.88	z	0.3252	113.6843	66.9987	70.1911	250.8741
8 ¹ B ₂	5d _{xz} -R	7.93	y	0.0127	184.2486	67.3410	173.6527	425.2423
9 ¹ A ₁	5d _{xy} -R	7.99	z	0.0814	161.1558	144.0513	66.2029	371.4099
12 ¹ B ₁	4d'-R	8.02	x	0.0001	105.1475	189.7472	184.0334	478.9280
9 ¹ B ₂	4d' _{xy} -R	8.14	y	0.0445	198.4062	188.6370	71.1856	458.2288
10 ¹ A ₁	4d' _{xz} -R	8.20	z	0.0758	195.4445	73.8492	177.7282	447.0220
10 ¹ B ₂	V-mix	8.25	y	0.2553	69.5117	56.0848	33.4018	158.9982
11 ¹ A ₁	5'p _x -R	8.32	z	0.0014	398.9488	141.0667	139.6109	679.6265
1 ³ B ₂	V	4.58			26.7894	20.9241	19.4356	67.1491
1 ³ A ₂	3s-R	5.08			38.9417	31.5646	42.5046	113.0110
1 ³ A ₁	V	5.60			27.3228	22.2646	18.8990	68.4864
1 ³ B ₁	3p _y -R	5.82			40.0917	67.9226	34.3289	142.3432

^aV and R denote, respectively, the valence and Rydberg excited state. For details see the text.^bTransition energy.^cPolarization direction of the transition moment.

$\rightarrow 3p_x, \pi^*, 3d_{xz}$), 2 ¹B₂ (valence $1a_2 \rightarrow \pi^*, 3p_x, 3d_{xz}$) and 3 ¹B₂ ($1a_2 \rightarrow 3d_{xz}, \pi^*, 3p_x$) that are moderately separated in energy. Thus, an attempt to assign pure Rydberg or pure valence excitations in this case is meaningless. In our present calculations, we found that one valence transition configuration, $1a_2 \rightarrow \pi^*$ (18 \rightarrow 52), is included in all three ¹B₂ states, and its contributions (absolute value of the coefficient of configuration) to the three ¹B₂ states are 0.35, 0.48 and 0.53, respectively. This further shows that the intensity of this energy region can be attributed mostly to valence excitation,

and explains why Rydberg transitions ($1a_2 \rightarrow 3p_x, \pi^*, 3d_{xz}$ and $1a_2 \rightarrow 3d_{xz}, \pi^*, 3p_x$) show strong intensity in this energy region. Our present calculated excitation energies, oscillator strengths, and second moments for the three ¹B₂ states are very similar to those by CC3 calculations. Assignment of the first ¹B₂ valence excitation in this energy region has been controversial in other theoretical studies.^{22,24,25,26,29} Although the 2 ¹B₂ state was calculated and assigned to be the valence excitation and was the major source of intensity for this energy region in CASPT2²² and MRMP²⁵ studies,

TABLE VI. SAC–CI results compared with the experimental excitation energies (in eV) and other theoretical results for pyrrole.

State	SAC	SAC–CI		Expt. ^c	CASPT2 ^d		MRMP ^e	ADC(2) ^f		CC3 ^g	
	Nature ^a	$f(r)$	ΔE^b		ΔE	Nature	ΔE	ΔE	Nature	ΔE	Nature
1 ¹ A ₂	3s–R	Forbid	5.11	~5.22	5.08	1 ¹ A ₂ -3s	4.92	5.03	3s(¹ A ₂)	5.20	3s(¹ A ₂)
1 ¹ B ₁	3p _y –R	0.0211	5.80	~5.7	5.85	1 ¹ B ₁ -3p	5.70	5.68	3p(¹ B ₁)	5.95	3p _y (¹ B ₁)
2 ¹ A ₂	3p _z –R	Forbid	5.81		5.83	2 ¹ A ₂ -3p	5.74	5.71	3p(¹ A ₂)	5.94	3p _z (¹ A ₂)
1 ¹ B ₂	3p _x –R/V	0.0805	5.88	~5.86	5.78	1 ¹ B ₂ -3p	5.87	5.86	3p(¹ B ₂)	6.04	3p _x (¹ B ₂)
2 ¹ B ₁	3s'–R	0.0005	6.05		5.97	2 ¹ B ₁ -3s'	5.81	5.77	3s'(¹ B ₁)	6.12	3s'(¹ B ₁)
3 ¹ A ₂	3d–R	Forbid	6.38		6.40	3 ¹ A ₂ -3d	6.45	6.25	3d(¹ A ₂)	6.51	3d(¹ A ₂)
3 ¹ B ₁	3d _{yz} –R	0.0037	6.39	~6.42	6.42	3 ¹ B ₁ -3d	6.38	6.27	3d(¹ B ₁)	6.55	3d _{yz} (¹ B ₁)
2 ¹ A ₁	V	0.0002	6.41		5.92	2 ¹ A ₁ -V	5.98	6.66	V(¹ A ₁)	6.37	V(¹ A ₁)
4 ¹ A ₂	3d–R	Forbid	6.44		6.51	4 ¹ A ₂ -3d	6.44	6.37	3d(¹ A ₂)	6.57	3d(¹ A ₂)
2 ¹ B ₂	V/3d _{xz} –R	0.0475	6.48	6.2–6.5	6.00	2 ¹ B ₂ -V	6.51	6.48	3d(¹ B ₂)	6.57	V(¹ B ₂)
3 ¹ A ₁	3d _{xy} –R	0.0000	6.64		6.54	3 ¹ A ₁ -3d	6.52	6.54	3d(¹ A ₁)	6.87	3d _{xy} (¹ A ₁)
4 ¹ B ₁	3p _z '–R	0.0266	6.68	6.5–6.7	6.62	4 ¹ B ₁ -3p'	6.48	6.43	3p'(¹ B ₁)	6.82	3p _z '(¹ B ₁)
5 ¹ A ₂	4s–R	Forbid	6.71		6.71	4s(¹ A ₂)		6.55	4s(¹ A ₂)	6.92	4s(¹ A ₂)
3 ¹ B ₂	3d _{xz} –R/V	0.0789	6.76	6.78	6.53	3 ¹ B ₂ -3d	6.61	6.71	V(¹ B ₂)	6.90	3d _{xz} (¹ B ₂)
					7.31	6 ¹ A ₂ -3d'	7.25			6.97	3p _y '(¹ A ₂)?
4 ¹ A ₁	3p _x '–R	0.0146	6.86	7.0–7.1	6.65	4 ¹ A ₁ -3p'	6.62	6.42	3p'(¹ A ₁)	7.04	3p _x '(¹ A ₁)
5 ¹ B ₁	4p _y –R	0.0029	6.93	7.0–7.1				6.78	4p(¹ B ₁)	7.17	4p _y (¹ B ₁)
6 ¹ A ₂	4p _z –R	Forbid	6.95		6.77	5 ¹ A ₂ -3d'	6.70	6.78	4p(¹ A ₂)	7.16	4p _z (¹ A ₂)
4 ¹ B ₂	4p _x –R	0.0020	6.99	7.0–7.1				6.88	4p(¹ B ₂)	7.20	4p _x (¹ B ₂)
7 ¹ A ₂	4d–R	Forbid	7.11					6.98	4d(¹ A ₂)	7.34	4d(¹ A ₂)
8 ¹ A ₂	4d–R	Forbid	7.13					6.99	4d(¹ A ₂)	7.36	4d(¹ A ₂)
6 ¹ B ₁	4d _{yz} –R	0.0001	7.14					7.00	4d(¹ B ₁)	7.37	4d _{yz} (¹ B ₁)
5 ¹ A ₁	4d _{xy} –R	0.0041	7.26	~7.35				7.12	4d(¹ A ₁)	7.48	4d _{xy} (¹ A ₁)
7 ¹ B ₁	3d'–R	0.0018	7.26		7.39	6 ¹ B ₁ -3d'	7.23	6.97	3d'(¹ B ₁)	7.41	3d'(¹ B ₁)
5 ¹ B ₂	4d _{xz} –R	0.0119	7.26	~7.4	7.72	5 ¹ B ₂ -4d		7.14	4d(¹ B ₂)	7.48	4d _{xz} (¹ B ₂)
9 ¹ A ₂	5s–R	Forbid	7.27								
8 ¹ B ₁	3d'–R	0.0092	7.34		7.32	5 ¹ B ₁ -3d'	7.14	7.09	3d'(¹ B ₁)	7.47	3d'(¹ B ₁)
10 ¹ A ₂	5p _z –R	Forbid	7.44								
9 ¹ B ₁	5p _y –R	0.0048	7.44	~7.54						...	
6 ¹ B ₂	5p _x –R	0.0020	7.45							and more Ryds	
6 ¹ A ₁	3d' _{xz} –R	0.0679	7.49		7.36	5 ¹ A ₁ -3d'	7.20	7.23	3d'(¹ A ₁)	...	
7 ¹ B ₂	3d' _{xy} –R	0.0052	7.55	~7.7	7.43	4 ¹ B ₂ -3d'	7.36	7.26	3d'(¹ B ₂)		
10 ¹ B ₁	4s'–R	0.0000	7.63					7.24	4s'(¹ B ₁)		
11 ¹ B ₁	5d _{yz} –R	0.0002	7.75	~7.85							
7 ¹ A ₁	4' _{p_x} –R	0.0020	7.83	~7.95							
8 ¹ A ₁	V-mix	0.3252	7.88	7.5–8	7.46	6 ¹ A ₁ -V	7.48	7.75	V(¹ A ₁)	7.91	V(¹ A ₁)
8 ¹ B ₂	5d _{xz} –R	0.0127	7.93	~8.0							
9 ¹ A ₁	5d _{xy} –R	0.0814	7.99	~8.1						...	
12 ¹ B ₁	4d'–R	0.0001	8.02							and more Ryds	
9 ¹ B ₂	4d' _{xy} –R	0.0445	8.14							...	
10 ¹ A ₁	4d' _{xy} –R	0.0758	8.20		7.88	7 ¹ A ₁ -4d'					
10 ¹ B ₂	V-mix	0.2553	8.25							8.31	V(¹ B ₂)
11 ¹ A ₁	5' _{p_x} –R	0.0014	8.32								
1 ³ B ₂	V		4.58	4.2	4.21			4.59			
1 ³ A ₂	3s–R		5.08		5.04			5.00			
1 ³ A ₁	V		5.60	5.10	5.16			5.55			
1 ³ B ₁	3p _y –R		5.82		5.82			5.63			

^aV and R denote, respectively, valence and Rydberg excited state. For details see the text.

^bTransition energy.

^cExperimental data are taken from Refs. 3, 7, 9, and 22, and references therein. Those for valence excitations are chosen as the bands' maximum; those for Rydberg transitions are 0–0 excitation energies.

^dReference 21.

^eReference 23.

^fReference 24.

^gReference 25.

the difference in the calculated vertical excitation energy of the 2 ¹B₂ state between CASPT2 and MRMP studies is as large as 0.51 eV. In recent ADC(2) studies,²⁶ however, the first ¹B₂ valence excitation was suggested to be outside this energy region, and the intensity for this region was ascribed mostly to the 1a₂→3p(¹B₂) Rydberg transition.

A weak singlet excited state has been observed at about

5.22 eV and assigned to one ¹A₁ state in the VUV absorption spectrum by Mullen and Orloff.³ However, this assignment was disputed by Robin¹⁵ and experimentally assigned to a Rydberg state. The present calculations compute the 1 ¹A₂ state with 1a₂→3s nature at 5.11 eV, which supports the notion that the lowest singlet state might be due to the vibrational structure of the dipole-forbidden 1a₂→3s Rydberg

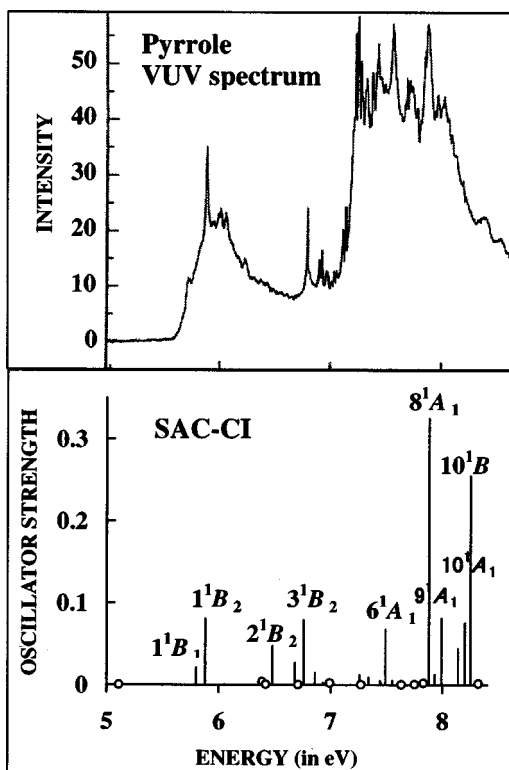


FIG. 4. VUV spectrum and SAC-CI theoretical spectrum of pyrrole.

transition, since the present calculations, together with previous high-level calculations,^{22,26,29} show that there is no other singlet state in this energy region.

Next, we discuss the valence excitation, $V'(^1A_1)$, which is expected to occur in the first band. As we discussed for the 2^1A_1 state of furan, a similar situation occurs in the 2^1A_1 state of pyrrole. Our present calculations give the 2^1A_1 state at 6.41 eV with an oscillator strength of 0.0002. Its second moment $\langle r^2 \rangle$ is 73.3451 a.u.², which clearly characterizes it as a valence excited state, and its nature is a mixture of $\pi_2-\pi^*$ ($17\rightarrow 52$) and $\pi_3-\pi^*$ transitions ($18\rightarrow 53$) and ($18\rightarrow 66$). Double excitation makes a rather small contribution. CC3 computed it to be 6.37 eV with an oscillator strength of 0.001. ADC(2) computed this state at 6.66 eV with an oscillator strength of 0.017. CASPT2 computed the 2^1A_1 state at 5.92 eV with an intensity of 0.0195, and its nature was reported to be a mixture of the single excitation

$2b_1\rightarrow 3b_1$ and $1a_2\rightarrow 2a_2$ configurations in combination with a large fraction (25%) of double excitations $(1a_2)^2\rightarrow (3b_1)^2$. MRMP computed this state at 5.98 eV with an intensity of 0.0098, and its nature was almost the same as that of CASPT2. Note that here there is again a discrepancy between SAC-CI, CC3, and CASPT2, MRMP results. However, in the case of thiophene, which will be discussed in a later paper,⁴³ the 2^1A_1 state (lowest excited state) has been well characterized to be predominantly single excitation by both SAC-CI and CASPT2 with regard to both excitation energy and oscillator strength, in good accordance with the experimental data of the VUV and magnetic circular dichroism spectra. Generally speaking, the SAC-CI SD-R method used here, together with the CCSD/CC3 and EOM-CCSD(T) methods, is best applied to states that are largely single excitation in nature, and may give a relatively high excitation energy estimate for the state of significant doubly excited character. Therefore, the doubly excited characters of the 2^1A_1 states of this series of five-membered ring compounds deserve to be further investigated by the SAC-CI general-R method,⁴⁴ which is suitable for two- and many-electron processes.

In the VUV spectrum of Mullen and Orloff,³ absorption peaks are observed at around 5.71 and 5.88 eV, and a question arises as to whether these two absorption peaks represent two separate electronic transitions or one transition with an associated vibrational structure. In the later UV spectrum of Bavia *et al.*,⁷ absorption peaks were reported at around 5.82 and 5.86 eV, however, an obvious absorption peak at around 5.7 eV was ignored. In the latest VUV spectrum of Palmer *et al.*,²⁴ absorption peaks were reported at around 5.698 and 5.861 eV and assigned to the $1^1B_2(1a_2\rightarrow 3p_x)$ and $1^1B_1(1a_2\rightarrow 3p_y)$ states, respectively. The 5.861 eV transition is the most intense and shows obvious vibrational structures in the first band. Other nearby peaks, e.g., 5.82 and 5.88 eV, are interpreted as part of the vibrational structure of this transition. Palmer *et al.*,²⁴ by comparing this with the envelope of the first band in PES,⁵ confirmed that the 5.861 eV absorption arises from the excitation of a $1a_2\rightarrow 3p$ Rydberg state associated with IP₁ (8.21 eV). Our present calculations support this general experimental assignment, but the calculated excitation energy orders and oscillator strengths prefer the assignment of the 5.861 eV transition to $1^1B_2(1a_2\rightarrow 3p_x, \pi^*)$ and the 5.698 eV transition to

TABLE VII. Comparison of electronic transition mechanisms in pyrrole and furan.

Pyrrole						Furan					
State	Nature	ΔE	$f(r)$	SM ^a	MC ^b	State	Nature	ΔE	$f(r)$	SM	MC
1^1A_1	Ground	0		-65.3		1^1A_1	Ground	0		-64.7	
1^1B_2	$3p_x-R\sim V$	5.88	0.081	-132.1	$1a_2-3p_x, 1a_2-\pi^*$	1^1B_2	V-mix	6.40	0.185	-92.5	$1a_2-\pi^*$
2^1A_1	V	6.41	0.000	-73.3	$2b_1-\pi^*, 1a_2-\pi^*$	2^1A_1	V	6.79	0.000	-69.0	$2b_1-\pi^*, 1a_2-\pi^*$
2^1B_2	$V-3d_{xz}-R$	6.48	0.048	-146.3	$1a_2-\pi^*, 1a_2-3d_{xz}$	2^1B_2	$3p_x-R$	6.82	0.016	-129.5	$1a_2-3p_x$
3^1B_2	$3d_{xz}-R\sim V$	6.76	0.079	-224.7	$1a_2-3d_{xz}, 1a_2-\pi$	3^1B_2	$3d_{xz}-R$	7.51	0.019	-245.7	$1a_2-3d_{xz}$
8^1A_1	V-mix	7.88	0.325	-250.9	$1a_2-\pi^*, 2b_1-\pi^*$	6^1A_1	V-mix	8.34	0.483	-97.5	$1a_2-\pi^*, 2b_1-\pi^*$
10^1B_2	V-mix	8.25	0.255	-159.0	$2b_1-\pi^*$	9^1B_2	V-mix	9.08	0.166	-130.4	$2b_1-\pi^*$

^aSM denotes second moment.

^bMC denotes main configuration.

$1^1B_1(1a_2 \rightarrow 3p_y)$, which is opposite the assignments of Palmer *et al.*²² Except for CASPT2, all previous theoretical studies, i.e., CC3, MRMP, and ADC(2), gave similar trends for excitation energy orders and oscillator strengths to our present results, however, all of them followed Bavia *et al.*⁷ and ignored the 5.7 eV peak, and assigned the 5.861 eV transition to $1^1B_2(1a_2 \rightarrow 3p_x)$ and the 5.82 or 5.88 eV transition instead of the 5.7 eV transition to $1^1B_1(1a_2 \rightarrow 3p_y)$.

The next peak in the VUV spectrum is observed at around 6.2 eV. This peak was assigned experimentally to the $2b_1 \rightarrow 3s$ Rydberg transition by Derrick *et al.*⁵ On the other hand, this peak, together with other peaks at slightly higher energies, was assigned experimentally to a vibrational structure of the $1a_2 \rightarrow 3p_x$ Rydberg state by Bavia *et al.*⁷ Our present calculations support an alternative assignment for this group of peaks, and associates them with the $V(2^1B_2)$ state calculated at 6.48 eV and its vibrational structure. Additionally, the $1a_2 \rightarrow 3d_{yz}$ (3^1B_1) Rydberg states, etc., are also predicted to be in this region. Note that the absorption peaks were reported at around 6.42 eV and assigned to the $1a_2 \rightarrow 3d$ Rydberg state in the UV spectrum of Bavia *et al.*⁷

2. The second weak central band (6.6–7.1 eV) in the VUV spectrum

A relatively intense absorption peak was observed at around 6.78 eV in the VUV spectrum by Palmer *et al.*,²⁴ and assigned to the $1a_2 \rightarrow 3d$ Rydberg transition instead of $1a_2 \rightarrow 4s$,⁷ which is dipole forbidden. Two other weaker bands at 7.021 and 7.044 eV were assigned to the excitations of the $2b_1 \rightarrow 3p$ series of Rydberg transitions.²⁴ Our present calculations support the above-given general assignments of this energy region. The 3^1B_2 state ($1a_2 \rightarrow 3d_{xz}$) is computed at 6.76 eV with an oscillator strength of 0.0789, which is the most intense absorption peak in this energy region and hence is reasonably associated with the absorption peak at around 6.78 eV in the VUV spectrum. It is easy to understand why this Rydberg transition is intense via the above-mentioned hybrid model. It is mixed with valence transition and hence it ‘‘borrows’’ the intensity from the valence transition. Most of the intensity of the first and second bands can be attributed to the same valence transition. Additionally, the $2b_1 \rightarrow 3p$ series of Rydberg states are also predicted in this region, and the $1a_2 \rightarrow 4p$ series of Rydberg states are predicted at the high-energy tail of this energy region. Note that CC3 calculations predicted very similar results in this energy region and also supported the assignment. However, CASPT2 and MRMP assigned the 6.78 eV peak to the $2b_1 \rightarrow 3p$ series of Rydberg transitions according to their calculations.

3. The third strong intense and broad band (7.1–8.2 eV) in the VUV spectrum

A strong intense and broad absorption superimposed with a few sharp peaks was observed at 7.1–8.2 eV in the VUV spectrum. Our present calculations computed the 8^1A_1 state at 7.88 eV with an oscillator strength of 0.3252 and the 10^1B_2 state at 8.25 eV with an oscillator strength of 0.2553. The nature of the 8^1A_1 state is a strong mixture of the $\pi \rightarrow \pi^*$ transitions ($18 \rightarrow 53$) and ($17 \rightarrow 52$) with the Rydberg transitions ($17 \rightarrow 26$) and ($18 \rightarrow 38$), etc., which are respon-

sible for the rather large second moment (250.9 a.u.²) of this state. The nature of the 10^1B_2 state is of strong mixture of $\pi \rightarrow \pi^*$ transitions ($17 \rightarrow 53$), ($17 \rightarrow 66$), and ($18 \rightarrow 52$) with Rydberg transition ($17 \rightarrow 27$), etc., which is responsible for the large second moment (159.0 a.u.²) of this state. The strong mixture of $\pi \rightarrow \pi^*$ excitations with Rydberg excitations reflects the strong interactions between valence and Rydberg excited states. Note that these interactions in pyrrole are stronger than those in furan. The two states mentioned previously are defined as energetically high valence states of A_1 and B_2 symmetries, respectively, considering oscillator strengths, main configurations, and second moments. Our present calculations show that a significant portion of the electronic absorption intensity in this region is due to the two energetically high valence excitations mentioned previously. We also predict that the $1a_2 \rightarrow 4d$ series, $1a_2 \rightarrow 5p$ series, $2b_1 \rightarrow 3d$ series, $1a_2 \rightarrow 5d$ series, $2b_1 \rightarrow 4d$ series, etc., Rydberg states are located in this energy region, and some of them have relatively large oscillator strengths. There are so many Rydberg states in only a 1 eV range, and therefore it is difficult to make an accurate assignment of Rydberg transitions in this energy region. For vibrational and geometrical relaxations, Rydberg transitions can easily overlap, and thus the absorption in this region becomes very complicated. However, we believe that it is reasonable to associate the valence and Rydberg excitations mentioned previously to the fine structure in the region 7.1–8.2 eV.

4. Triplet excited states

The two lowest triplet transitions of pyrrole have been identified by the electron energy-loss (EEL)^{8–10,24} spectrum at 4.2 and 5.1 eV, which are assigned to the 3^3B_2 and 3^3A_1 valence transitions, respectively. Our present calculations computed the 1^3B_2 state at 4.58 eV with a second moment of 67.1 a.u.², and the 1^3A_1 state at 5.60 eV with a second moment of 68.5 a.u.² The second moments of these two states (listed in Table V) clearly characterize them as valence excitations. The main configurations of 1^3B_2 are ($18 \rightarrow 52$), ($18 \rightarrow 62$), ($18 \rightarrow 59$), ($18 \rightarrow 64$), etc., and those of 1^3A_1 are ($17 \rightarrow 52$), ($18 \rightarrow 66$), ($18 \rightarrow 53$), ($17 \rightarrow 62$), etc. In the same energy region, we found two Rydberg excited states 1^3A_2 , 1^3A_1 and 1^3B_2 , which are given at 5.08 and 5.82 eV, respectively.

C. Comparison of furan and pyrrole

Comparing the present calculations of furan with those of pyrrole, it is obvious that a similar electronic excitation mechanism occurs in both molecules. There are two valence excitations in B_2 and A_1 symmetry, respectively, which are responsible for most of the intensity of the electronic absorption bands, and hence span the general profiles of the VUV spectra in the energy region up to around 8.2 eV in pyrrole and 8.8 eV in furan. From the main configurations listed in Table VII, we can see that both $1a_2$ and $2b_1$ series $\pi \rightarrow \pi^*$ valence transition configurations contribute to the two valence excitations of A_1 symmetry in both molecules. However, the $1a_2$ series $\pi \rightarrow \pi^*$ valence transition configurations predominantly contribute to the lowest valence excitation of

B_2 symmetry and the $2b_1$ series $\pi \rightarrow \pi^*$ predominantly contribute to the higher-energy valence excitation of B_2 symmetry in both molecules. At the same time, these valence excitations are more or less influenced by low-lying Rydberg transitions. In the case of pyrrole, due to the lower first ionization potential (IIPs), the Rydberg states are expected to be in the lower energy region, which is proven by our present calculations. In furan, the lowest excited state is the valence excitation of B_2 symmetry except for the dipole-forbidden $3s$ Rydberg transition, whereas in pyrrole the energies of the $3p$ series Rydberg transitions are lower than that of the lowest valence excitation of B_2 symmetry, which gives rise to stronger interactions between valence and Rydberg excitations than in furan. It is also clear from the second moments of these states that the interactions between valence and Rydberg transitions in pyrrole are much stronger than those in furan, which is responsible for the more complicated VUV fine structure of pyrrole.

Comparing the present SAC–CI results with those obtained by the CCSD and CC3 methods, we find that the general trends are very similar, and the difference in excitation energies is very small, less than 0.1 eV (maximum) for valence excitations and 0.25 eV (maximum) for Rydberg transitions. These similar results are natural since the basic theories are quite similar and the difference lies only in computational methodology: the former uses perturbation selection schemes and the latter adopts integral-direct strategies. The present results, comparing with CCSD/CC3 results, show that the perturbation selection scheme in the SAC–CI SD-R method is very effective and reserves a high accuracy at the same time.

IV. CONCLUSIONS

The SAC/SAC–CI theory was applied to furan and pyrrole to reinvestigate their electronic excited states in more detail, including the singlet and triplet valence and Rydberg excited states. The SAC/SAC–CI method with a sufficiently extended basis set and a large active space gave a quantitatively satisfactory result to make reliable assignments for the electron excitation spectrum of furan and pyrrole. The present results show good agreement with various experimental data measured by VUV and EEL spectroscopies. The mixing of valence and Rydberg states was stronger in pyrrole than in furan.

In the case of furan, four singlet valence $\pi-\pi^*$ excitations (two A_1 states and two B_2 states), which span the general profile of the VUV spectrum, agree well with the latest experimental data by Palmer *et al.*²³ In particular, our present results strongly support the notion that valence excitation exists in the 8.7 eV energy region. In addition, many Rydberg excitations were determined in the present calculations, and the corresponding assignments in this work should constitute a useful theoretical reference for experimental chemists in this field.

In the case of pyrrole, 43 low-lying singlet excited states were obtained theoretically and reliable assignments for the VUV spectrum up to 8.2 eV were made using the calculated energies and oscillator strengths. Valence and Rydberg excited states were discussed separately in detail. For the first

intense band and second weak band of the VUV spectrum, our present calculated results show a strong mixture of valence and Rydberg excitations in the first three 1B_2 excited states. For the third strong and broad band, the present calculations give two valence excited states, 8^1A_1 and 10^1B_2 , which are strongly influenced by Rydberg transitions. These valence excitations, together with Rydberg excitations, span the general profile of the VUV spectrum observed by Palmer *et al.*²⁴

ACKNOWLEDGMENTS

This research was supported by a Grant-in-Aid for Scientific Research from the Ministry of Education, Science, Culture and Sports. The authors are grateful to K. Toyota for helpful discussions on this subject.

- ¹W. C. Price and A. D. Walsh, Proc. R. Soc. London, Ser. A **179**, 201 (1941).
- ²L. W. Pickett, N. J. Hoeflich, and T.-C. Liu, J. Am. Chem. Soc. **73**, 4865 (1951).
- ³P. A. Mullen and M. K. Orloff, J. Chem. Phys. **51**, 2276 (1969).
- ⁴J. H. D. Eland, J. Mass Spectrom. Ion Phys. **2**, 471 (1969).
- ⁵P. J. Derrick, L. Asbrink, O. Edqvist, B.-O. Jonsson, and E. Lindholm, Int. J. Mass Spectrom. Ion Phys. **6**, 161 (1971).
- ⁶P. J. Derrick, L. Asbrink, O. Edqvist, and E. Lindholm, Spectrochim. Acta A **27**, 2525 (1971).
- ⁷M. Bavia, F. Bertinelli, C. Taliani, and C. Zauli, Mol. Phys. **31**, 479 (1976).
- ⁸W. M. Flicker, O. A. Mosher, and A. Kuppermann, J. Chem. Phys. **64**, 1315 (1976).
- ⁹W. M. Flicker, O. A. Mosher, and A. Kuppermann, Chem. Phys. Lett. **38**, 489 (1976).
- ¹⁰E. H. Van Veen, Chem. Phys. Lett. **41**, 535 (1976).
- ¹¹B. Norden, R. Hakansson, P. B. Pedersen, and E. W. Thulstrup, Chem. Phys. **33**, 355 (1978).
- ¹²C. D. Cooper, A. D. Williamson, J. C. Miller, and R. N. Compton, J. Chem. Phys. **73**, 1527 (1980).
- ¹³J. L. Roebber, D. P. Gerrity, R. Hemley, and V. Vaida, Chem. Phys. Lett. **75**, 104 (1980).
- ¹⁴L. Nyulaszi, J. Mol. Struct. **273**, 133 (1992).
- ¹⁵M. B. Robin, *Higher Excited States of Polyatomic Molecules* (Academic, New York, 1975), Vol. II.
- ¹⁶K. Tanaka, T. Nomura, T. Noro, H. Tatewaki, T. Takada, H. Kashiwagi, F. Sasaki, and K. Ohno, J. Chem. Phys. **67**, 5738 (1977).
- ¹⁷W. Butscher and K.-H. Thunemann, Chem. Phys. Lett. **57**, 224 (1978).
- ¹⁸K.-H. Thunemann, R. J. Buenker, and W. Butscher, J. Chem. Phys. **47**, 313 (1980).
- ¹⁹D. C. Rawlings and E. R. Davidson, Chem. Phys. Lett. **98**, 424 (1983).
- ²⁰D. C. Rawlings, E. R. Davidson, and M. Gouterman, Int. J. Quantum Chem. **26**, 237 (1984).
- ²¹H. Nakatsuji, O. Kitao, and T. Yonezawa, J. Chem. Phys. **83**, 723 (1985).
- ²²L. Serrano-Andres, M. Merchán, I. Nebot-Gil, B. O. Roos, and M. Fulscher, J. Am. Chem. Soc. **115**, 6184 (1993).
- ²³M. H. Palmer, I. C. Walker, C. C. Ballard, and M. F. Guest, Chem. Phys. **192**, 111 (1995).
- ²⁴M. H. Palmer, I. C. Walker, and M. F. Guest, Chem. Phys. **238**, 179 (1998).
- ²⁵H. Nakano, T. Tsuneda, T. Hashimoto, and K. Hirao, J. Chem. Phys. **104**, 2312 (1996).
- ²⁶A. B. Trofimov and J. Schirmer, Chem. Phys. **214**, 153 (1997).
- ²⁷A. B. Trofimov and J. Schirmer, Chem. Phys. **224**, 175 (1997).
- ²⁸O. Christiansen and P. Jørgensen, J. Am. Chem. Soc. **120**, 3423 (1998).
- ²⁹O. Christiansen, J. Gauss, J. Stanton, and P. Jørgensen, J. Chem. Phys. **111**, 525 (1999).
- ³⁰Landolt-Bornstein, *Numerical Data and Functional Relationships in Science and Technology, New Series, Group II: Atomic and Molecular Physics*, Structure Data of Free Polyatomic Molecules, Vol. 7, edited by J. H. Callomon, E. Hirota, K. Kuchitsu, W. J. Lafferty, A. G. Maki, and C. S. Pote (Springer, Berlin, 1976).

- ³¹R. A. Kendall, T. H. Dunning, Jr., and R. J. Harrison, *J. Chem. Phys.* **96**, 6796 (1992).
- ³²T. H. Dunning, Jr., *J. Chem. Phys.* **90**, 1007 (1989).
- ³³K. Kaufmann, W. Baumeister, and M. Jungen, *J. Phys. B* **22**, 2223 (1989).
- ³⁴GAUSSIAN 98 (Revision A.1), M. J. Frisch, G. W. Trucks, H. B. Schlegel, G. E. Scuseria, M. A. Robb, J. R. Cheeseman, V. G. Zakrzewski, J. A. Montgomery, R. E. Stratmann, J. C. Burant, S. Dapprich, J. M. Millam, A. D. Daniels, K. N. Kudin, M. C. Strain, O. Farkas, J. Tomasi, V. Barone, M. Cossi, R. Cammi, B. Mennucci, C. Pomelli, C. Adamo, S. Clifford, J. Ochterski, G. A. Petersson, P. Y. Ayala, Q. Cui, K. Morokuma, D. K. Malick, A. D. Rabuck, K. Raghavachari, J. B. Foresman, J. Cioslowski, J. V. Ortiz, B. B. Stefanov, G. Liu, A. Liashenko, P. Piskorz, I. Komaromi, R. Gomperts, R. L. Martin, D. J. Fox, T. Keith, M. A. Al-Laham, C. Y. Peng, A. Nanayakkara, C. Gonzalez, M. Challacombe, P. M. W. Gill, B. G. Johnson, W. Chen, M. W. Wong, J. L. Andres, M. Head-Gordon, E. S. Replogle, and J. A. Pople, Gaussian, Inc., Pittsburgh, PA (1998).
- ³⁵H. Nakatsuji and K. Hirao, *J. Chem. Phys.* **68**, 2053 (1978).
- ³⁶H. Nakatsuji, *Chem. Phys. Lett.* **59**, 362 (1978).
- ³⁷H. Nakatsuji, *Chem. Phys. Lett.* **67**, 329 (1979).
- ³⁸H. Nakatsuji, *Computational Chemistry: Reviews of Current Trends*, edited by J. Leszczynski (World Scientific, Singapore, 1997), Vol. 2.
- ³⁹K. Hirao and H. Nakatsuji, *Chem. Phys. Lett.* **79**, 292 (1981).
- ⁴⁰H. Nakatsuji, *Chem. Phys.* **75**, 425 (1983).
- ⁴¹H. Nakatsuji, M. Hada, M. Ehara, J. Hasegawa, T. Nakajima, H. Nakai, O. Kitao, and K. Toyota, SAC/SAC-CI program system (SAC-CI96) for calculating ground, excited, ionized, and electron attached states and singlet to septet spin multiplicities.
- ⁴²J. Wan, M. Ehara, M. Hada, and H. Nakatsuji, *J. Chem. Phys.* (to be published).
- ⁴³J. Wan, M. Hada, M. Ehara, and H. Nakatsuji (unpublished).
- ⁴⁴H. Nakatsuji, *Chem. Phys. Lett.* **59**, 331 (1991).